www.czasopisma.pan.pl PAN www.journals.pan.pl
Opto-Electronics Review 26 (2018) 195–200

Contents lists available at ScienceDirect

Opto-Electronics Review

journal homepage: http://www.journals.elsevier.com/opto-electronics review

Full Length Article

Nanostructures with Ge–Si quantum dots for infrared photodetectors

I.I. Izhnin [a], O.I. Fitsych [a], A.V. Voitsekhovskii [b], A.P. Kokhanenko [b], K.A. Lozovoy [b,*], V.V. Dirko [b]

[a] Scientific Research Company "Carat", Stryjska St. 202, Lviv 79031, Ukraine
[b] National Research Tomsk State University, Lenin Av. 36, Tomsk 634050, Russia

ARTICLE INFO

Article history:
Received 15 January 2018
Received in revised form 10 April 2018
Accepted 9 June 2018
Available online 30 June 2018

Keywords:
Molecular beam epitaxy
Heterostructures
Dark current
Noise
Detectivity

ABSTRACT

In this paper questions of optimization of growth conditions in the method of molecular beam epitaxy for creation of high-efficient quantum dot infrared photodetectors are considered. As a model material system for theoretical investigations, heterostructures with germanium-silicon quantum dots on the silicon surface are chosen. For calculations of the dependencies of quantum dots array parameters on synthesis conditions the kinetic model of growth of differently shaped quantum dots based on the general nucleation theory is proposed. The theory is improved by taking into account the change in free energy of nucleation of an island due to the formation of additional edges of islands and due to the dependence of surface energies of facets of quantum dots on the thickness of a 2D wetting layer during the Stranski–Krastanow growth. Calculations of noise and signal characteristics of infrared photodetectors based on heterostructures with quantum dots of germanium on silicon are done. Dark current in such structures caused by thermal emission and barrier tunneling of carriers, as well as detectivity of the photodetector in the approximation of limitation by generation-recombination noises are estimated. Moreover, the presence of dispersion of quantum dots by size is taken into account in the calculations of the generation-recombination noises. Results of calculations of the properties of structures with quantum dots and their dependencies on growth parameters, as well as the characteristics of quantum dot photodetectors are presented. Comparison of the estimated parameters of quantum dots ensembles and the characteristics of quantum dot photodetectors with experimental data is carried out.

1. Introduction

Researchers pay great attention to creation of various electronic devices based on the structures with quantum dots of germanium on silicon since early 1990's, when they were obtained in the experiments [1,2] by the method of molecular beam epitaxy (MBE) for the first time. There are infrared photodetectors, fast-speed transistors and solar cells among these devices [3–5]. Such a high interest to the Ge-Si heterostructures with quantum dots is due to the number of unique properties of these structures caused by the effects of size quantization [6–8]. These new phenomena appearing in the structures with quantum dots make them attractive to device application [9,10].

Infrared photodetectors may be used in the wide range of various applications: for military and civil needs, in energetics, medicine, and industry. Photodetectors are required to have high operating characteristics (such as sensitivity and detectivity), to operate at high temperatures, and to have a reasonably low price. To date, the basic material for creation of infrared photodetectors is mercury-cadmium telluride (MCT). However, there are some technological difficulties connected with the synthesis of MCT epitaxial layers. And now quantum dot infrared photodetectors may become good alternative to traditional MCT detectors [11–13].

Principles of quantum dot infrared photodetectors operation are analogous to those of quantum well infrared photodetectors. The principal difference is only the restriction in all three dimensions of the charge carrier motion in a quantum dot [14]. It is expected that due to this restriction quantum dot photodetectors will provide better characteristics, namely higher operating temperatures, lower dark currents and higher photoelectric gains [13]. Finally, that may result in higher response and detectivity [15].

To date, not all the potential advantages of photodetectors with quantum dots are realized. It may be explained both by low degree of islands homogeneity in the array, and by non-optimal energy structure of such detectors. For example, quantum dots may have additional energy levels located between the ground and excited states, which are responsible for the absorption of the radiation of

* Corresponding author.
E-mail addresses: i.izhnin@carat.electron.ua (I.I. Izhnin), o.fitsych@ukr.net (O.I. Fitsych), vav43@mail.tsu.ru (A.V. Voitsekhovskii), kokh@mail.tsu.ru (A.P. Kokhanenko), lozovoymailbox@gmail.com (K.A. Lozovoy), vovenmir@gmail.com (V.V. Dirko).

https://doi.org/10.1016/j.opelre.2018.06.002
1230-3402/

the given wavelength. Moreover, the excited energy level may be rather distant from the conduction band and high applied biases are required. These factors increase dark current and decrease absorption coefficient. Finally, they lessen detectivity of quantum dot photodetectors compared with the predicted ultimate characteristics [11].

The most perspective method of quantum dots creation is molecular beam epitaxy. This method is based on the effects of self-organization of semiconductor nanostructures in heteroepitaxial systems. For various applications it is necessary to create heterostructures with quantum dots with different properties. These properties are defined by such parameters of quantum dots as their shape, average size, size distribution function and surface density. So, the important task is to estimate optimum growth conditions for obtaining heterostructures with given properties.

The aim of this paper was the calculation of noise characteristics of quantum dot photodetectors, firstly, taking into account generation-recombination noises, and, secondly, with the respect to the dispersion of quantum dots in array by sizes, for the further optimization of growth conditions in the method of molecular beam epitaxy for creation of photodetectors with improved detectivity.

2. Methods

Dark current of a photodetector is the current caused by various sources other than by incident signal flux (for example, background radiation or thermal generation of carriers). It is well known, that the dark current of a quantum dot photodetector is mainly caused by the processes of the thermal generation of carriers and barrier tunneling in the presence of the electric field. In this case dark current density may be written as [16]:

$$j_d = 2q(2\pi m^* K_B T/h^2)^{3/2}\exp(-E_a/K_B T)\mu F[1+(\mu F/v_s)^2]^{-1/2}, \quad (1)$$

where q is the electron charge, m^* is the effective mass of charge carrier in barrier layer, K_B is the Boltzmann's constant, T is the temperature, h is the Planck's constant, E_a is the activation energy, F is the applied electric field, μ is the mobility and v_s is the maximum carrier speed.

Activation energy may be written as the sum of two contributions from two different mechanisms of generation of carriers [17]:

$$E_a = E_{0,m}\exp(-F/F_0) + E_{0,n} - \alpha F, \quad (2)$$

where $E_{0,m}$ and $E_{0,n}$ are the activation energies at zero bias for two different mechanisms of carrier transport – microscopic and nanoscale [18]. The activation energy $E_{0,m}$ is defined as the difference between the Fermi level and the lowest energy level in conduction band of barrier layer. This value corresponds to the processes of the thermal emission. The activation energy $E_{0,n}$ is equal to ionization energy of a quantum dot. This energy describes barrier tunneling of carriers. F_0 and α are the fitting parameters characterizing the rate of energy change with applied bias [13].

Due to the inevitable existence of size inhomogeneity between quantum dots in the ensemble, activation energy of tunneling processes changes from one dot to another and it may be described by the Gaussian distribution with the dispersion σ_E^2. The value of σ_E determines the spread in activation energies $E_{0,n}$ caused by size inhomogeneity of the islands. Taking into account this distribution an average dark current density of the photodetector can be written as [13]:

$$j_d = q\mu F[1+(\mu F/v_s)^2]^{-1/2}(2\pi m^* K_B T/h^2)^{3/2} \exp(-(E_{0,m}\exp(-F/F_0) + E_{0,n} - \alpha F - \sigma_E^2/2K_B T)/K_B T)\mathrm{erfc}(-(E_{0,n} - \sigma_E^2/2K_B T)/\sigma_E(2)^{1/2}). \quad (3)$$

For the calculation of quantum dot array parameters, such as the average size L_{av}, the size dispersion δL and the surface density of quantum dots N, the kinetic model of growth of Ge quantum dots on Si [19–22] was used. This model is based on a generalization of the classical nucleation theory and allows one to define the dependencies of quantum dots surface density and size distribution function on growth temperature and deposition rates. For the modelling of quantum dots growth, first of all, such thermodynamic parameters of the Ge/Si system as change in free energy during transition from 2D to 3D growth and equilibrium thickness of the wetting layer were defined [23–25]. Free energy change due to elastic strain relaxation, formation of the additional edges, increase in the surface of the facets and decrease of atoms attraction to the substrate were considered. Moreover, surface energy dependence on the thickness of the deposited material was taken into account. The change in the free energy $\Delta F(i)$ during the transition of i atoms from the wetting layer to an island may be written as a sum of three summands [25]:

$$\Delta F(i) = Ai^{2/3} - B\zeta i + Ci^{1/3}, \quad (4)$$

where $\zeta = h / h_{eq} - 1$ is the wetting layer superstress, h is the Ge wetting layer thickness, h_{eq} is the equilibrium thickness of the wetting layer at which the transition of atoms from the wetting layer to an island becomes energetically favourable. According to the Muller–Kern criterion [26], for the wetting layer thicknesses $h < h_{eq}$ layer-by-layer growth takes place. If $h < h_{eq}$, the 2D to a 3D transition is observed which results in the reduction of free energy [20]. A, B, and C are the parameters depending on the growth temperature and the thermodynamic properties of the materials and characterizing surface energy increase, elastic strain relaxation, and change in the free energy due to the formation of the additional edges, correspondingly.

The equilibrium thickness of the wetting layer h_{eq} may be found by solving the following equation [27]:

$$[1-Z(\varphi)]\lambda\varepsilon_0^2 - 1/d_0\{\gamma_s - [\gamma(0,0) - \gamma(0,\infty)] \exp(-B_0 h_{eq}/d_0) - \gamma(0,\infty)\}\exp(-h_{eq}/k_0 d_0) = 0, \quad (5)$$

where $Z(\varphi)$ is the coefficient of elastic strain relaxation [28–30], φ is the contact angle of quantum dot, λ is the material's modulus of elasticity, ε_0 is the lattices' mismatch, d_0 is the height of one monolayer (ML), γ_s is the specific surface energy of the substrate, k_0 is the relaxation coefficient. $\gamma(\varphi, 0)$ and $\gamma(\varphi, \infty)$ are the specific surface energies of a facet with the contact angle φ on the surface of pure silicon (without the wetting layer) and on the surface of pure strained germanium (infinite wetting layer thickness) respectively [20,26,31–33], B_0 is the dimensionless parameter characterizing the rate of specific surface energy change with the deposited material thickness [34–38].

Then, islands nucleation rate, surface density of quantum dots, rate of atoms arrival to an island, the critical thickness of the wetting layer h_c and quantum dots size distribution function are calculated [21–25].

When considering the contribution of the edges to the free energy of the atoms in an island, to determine the critical thickness h_c of the transition from two-dimensional to three-dimensional growth, it is necessary to solve the following equation for the critical superstress $\zeta_c = (h_c / h_{eq} - 1)$ [25]:

$$4h_{eq}\zeta_c/(6(\pi)^{1/2}d_0 a(\zeta_c+1)F(\zeta_c))[2F(\zeta_c)\tau_{inc} /\zeta_c^2 t_{eq}]^{5/2}\exp[F(\zeta_c)] = 1, \quad (6)$$

where $t_{eq} = h_{eq} / V$ is the growth time for the wetting layer of the equilibrium thickness, V is the growth rate, $\zeta_c = (h_c / h_{eq} - 1)$ is the critical superstress, i_c is the critical number of atoms in an island, at which the function of the free energy $\Delta F(i)$ reaches its maxi-

mum, $F(\zeta_c)$ is the nucleation activation barrier $\Delta F(i_c)$ at $\zeta = \zeta_c$, τ_{inc} is the characteristic time of atoms incorporation processes at the boundary of an island, and a is the parameter defined as:

$$a = 3i_c^{1/3}(|\Delta F''(i_c)|/2\pi)^{1/2}/2\zeta. \quad (7)$$

Quantum dots size distribution function $f(L)$ in this case is given by [39]:

$$f(L) = 4L\Delta F(\zeta_c)\tau_{inc}\mathrm{Nexp}[2\Delta F(\zeta_c)\tau_{inc}(L_{av}^2-L^2)/\zeta_c^2 t_{eq}(\alpha_g l_0)^2 - \exp(2\Delta F(\zeta_c)\tau_{inc}(L_{av}^2-L^2)/\zeta_c^2 t_{eq}(\alpha_g l_0)^2)]/\zeta_c^2 t_{eq}(\alpha_g l_0)^2, \quad (8)$$

where α_g is the geometrical factor depending on the shape of quantum dot, l_0 is the mean distance between atoms at the wetting layer surface, L_{av} is the average lateral size of the dots [21–25].

For the description of the Ge_xSi_{1-x} layers deposition on the silicon surface it is essential to take into account in the formulae above the dependences of the thermodynamic parameters on the composition x. For this purpose the values of the physical constants for pure materials (Si, Ge) and the Vegard's law are used [40].

3. Results and discussion

For calculations of the characteristics of an ensemble of quantum dots we used the following values for the parameters of the model [20,24,25,34–36,41]: $l_0 = 0.395$ nm, $d_0 = 0.145$ nm, $\lambda = 1.27*10^{12}$ dyn/cm^2, $\varepsilon_0 = 0.042$, $\Psi_0 = 450$ erg/cm^2, $\varphi = 20°$, $\nu = 10$, $D(T_g) = 10^{-4}*\exp(-1.21 / k_B T_g)$ cm^2/s, $\gamma_s = 1260$ erg/cm^2, $\gamma(0, 0) = 1450$ erg/cm^2, $\gamma(0, \infty) = 1000$ erg/cm^2, $\gamma(\varphi, 0) = 1440$ erg/cm^2, $\gamma(\varphi, \infty) = 920$ erg/cm^2, $B_0 = 1.02$, $B_\varphi = 0.85$, $k_0 = 0.8$, $\beta = 1.5*10^{-6}$ erg/cm. Square-based pyramidal quantum dots were considered everywhere in the calculations.

Equation (5) has been solved numerically for the Ge/Si(001) material system in order to find the equilibrium wetting layer thickness h_{eq} for the Stranski–Krastanow growth of quantum dots in this system [27]. As a result, for the equilibrium wetting layer thickness with the use of the listed above parameters the value $h_{eq} = 2.5$ ML was obtained. This value corresponds to the results of a number of experiments on growth of quantum dots in the Ge/Si(001) system [2,27,32,42,43].

Found from solving Eq. (6), the critical thickness of the transition from 2D to 3D growth becomes larger compared to its estimation without considering the contribution of additional edge energy. For example, at the growth temperature $T_g = 500$ °C and the germanium deposition rate $V = 0.07$ ML/s, the critical thickness increases from 4.7 to 5.2 ML when accounting for the energy of edge formation [25,44].

The omparison of the calculated values of the critical thickness of 2D-3D transition in the Ge_xSi_{1-x}/Si system for different compositions at the growth temperature $T_g = 600$ °C and the growth rate $V = 0.17$ ML/s is represented in Fig. 1. Results of estimations exhibit good agreement with the experimental data [44].

It is worth mentioning that existing theoretical models try to explain the indicated phenomena with the help of segregation effect [45]. In these models the distribution of the concentration of germanium and silicon atoms over near-surface monolayers due to the phenomenon of the segregation is determined on the basis of the equations for the thermal activation exchange of atoms, and then the elastic stress energy is calculated with allowance for all the deposited layers. As a condition for achieving the critical thickness of the Stranski-Krastanow transition, the equality of changes in the energy of the system is chosen as a result of the relaxation of elastic stresses in the island and increasing the surface energy with the formation of additional faces [45]. However, these models are incapable of explaining the observed temperature dependence of the critical thickness and give good agreement with experiments only in the range of high growth temperatures [40]. Comparison

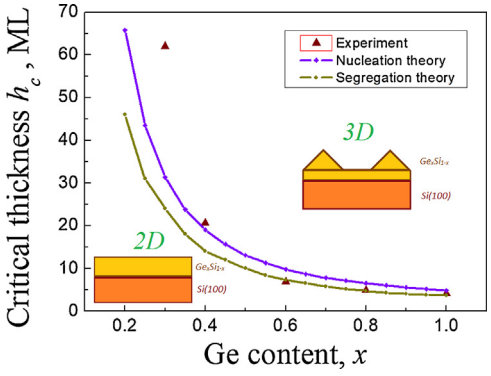

Fig. 1. Comparison of the experimental [44] and calculated values of the critical thickness for different compositions at $T_g = 600$ °C in the frames of nucleation theory (♦, this work) and segregation theory (●, [45]).

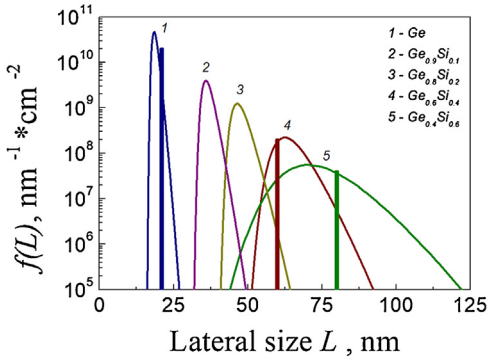

Fig. 2. Dependences of quantum dots size distribution function on the composition x for the growth temperature $T_g = 600$ °C and corresponding experimental data on the average sizes of quantum dots (bars) for Ge contents $x = 1.0, 0.6, 0.4$ [46–48].

of the calculated results obtained by these two methods (nucleation and segregation theories) is also presented in Fig. 1. It is obvious that nucleation theory (this work) describes the experimental results better than segregation theory [45] which does not take into account change in free energy of island's nucleation due to the formation of additional edges of islands and due to the dependence of surface energies of facets of quantum dots on the thickness of 2D wetting layer.

Further, such parameters of quantum dots ensemble as surface density and size distribution function for various Ge contents x in Ge_xSi_{1-x}/Si system were estimated (Fig. 2). The bars in Fig. 2 show the experimental data on the mean lateral size of quantum dots [46–48] for the compositions $x = 1.0$, 0.6, and 0.4, the growth rate $V = 0.04$ ML/s and the growth temperature $T_g = 600$ °C. In compliance with Fig. 2, with decrease in germanium content from $x = 1$ to $x = 0.4$ the average size of quantum dots increases approximately by 3 times, while their surface density decreases approximately by 1 order of magnitude [40].

The calculations of dark current and detectivity were done for the quantum dots arrays with the average sizes of 10, 15, and 20 nm. Results of the modelling show that with growth temperature increasing quantum dots sizes dispersion decreases and the detectivity slightly grows. So, greater values of the detectivity may be achieved in the photodetectors based on the nanoheterostructures with quantum dots grown at 500 °C and higher temperatures and corresponding high Ge deposition rates [39].

With the help of the obtained expressions estimations of the dark current and detectivity for the photosensitive structures based on silicon with germanium quantum dots were carried out. For the calculations the following model parameters were used [9,13,14]: $E_{0,m} = 60$ meV, $E_{0,n} = 300$ meV, $F_0 = 4$ kV/cm,

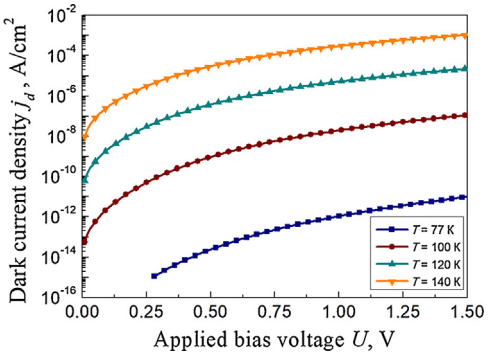

Fig. 3. Dark current density in Ge/Si quantum dot photodetectors as a function of applied bias U for σ_E = 10 meV at different operating temperatures T.

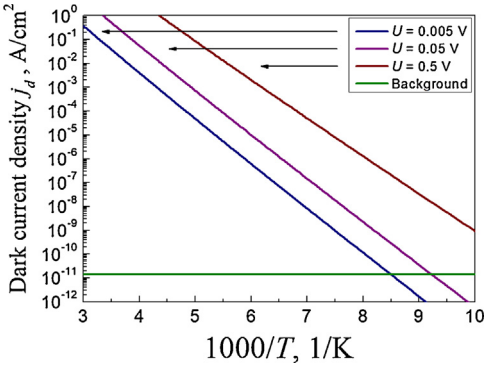

Fig. 4. Temperature dependence of dark current density for Ge/Si quantum dot photodetectors for σ_E = 10 meV and various applied biases U, as well as dark current density in the case of background limited performance (for the background temperature 77 K).

α = 2 meV·cm/kV, μ = 1000 cm^2/(V·s), $v_s = 10^7$ cm/s, $m^* = 0.56m_e$, $m_e = 9.1\cdot10^{-31}$ kg. The dependencies of the dark current on the operating temperature, applied bias and the value of dispersion in activation energies of transport processes due to barrier tunneling were determined.

Figure 3 represents dark current-voltage characteristics of the photodetector with quantum dots of Ge on Si with the above stated parameters for different operating temperatures and the value of energy dispersion σ_E = 10 meV, that is approximately 3% from the full activation energy E_a at zero bias.

As it is seen from Fig. 3, for low biases the dark current sharply grows with the increase of the applied electrical field. For example, for the temperature T = 100 K dark current density increases from $5.9\cdot10^{-13}$ A/cm^2 at U = 0.05 V to $9.4\cdot10^{-10}$A/cm^2 at U = 0.5 V. Then (at biases U > 0.5 V), with the increase of applied electrical field the dark current grows more slowly. Such a behaviour of the curves is explained by the co-existence of two excitation mechanisms of dark carriers. Thermal emission processes described by $E_{0,m}$ activation energy dominate for the weak electrical fields. With increase of applied bias the probability of ionization processes due to the barrier tunneling in strong fields increases [13,18].

Figure 4 shows temperature dependence of dark current density for quantum dot photodetector based on Ge/Si nanostructures with the stated above parameters for various applied biases U and energy dispersion σ_E = 10 meV.

In accordance with Fig. 4 the dark current of the photodetector strongly depends on the operating temperature. At the temperatures near 100 K dark current density is about 10^{-12} A/cm^2 for U = 0.05 V, while at room temperatures it may reach the value of 1 A/cm^2. For comparison, the dark current caused by background irradiation (for the background temperature 77 K) is also shown in Fig. 4. The dark current caused by background irradiation I_b was calculated by the general formula:

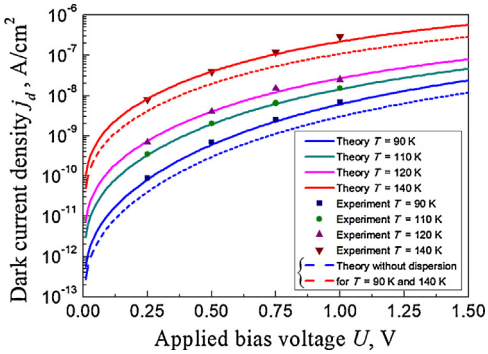

Fig. 5. Dark current-voltage characteristics of quantum dot photodetectors from the work [9] for various temperatures of the detector: T = 90, 110, 120 and 140 K. Theoretical curves corresponds to the results of calculations with respect to the dispersion of islands by sizes (solid lines) and without taking into account the inhomogeneity of islands (dash lines).

$$I_b^2 = 4q^2\eta\Phi_b A_d \Delta f, \tag{9}$$

where η is the quantum efficiency of the photodetector, $\Phi_b$is the density of background photon flux, $A_d$is the photosensitive area of the detector, Δf is the bandwidth.

For verification of the model comparison of the calculated values of the dark current with the experimental results obtained in Refs. 5, 9, 14, 49–51 were carried out. In Refs. 9 and 49 infrared photodetectors based on the heterostructures with germanium quantum dot layers in silicon matrix are described. The photodetectors studied were vertical p^+–p–p^+ structures with ten layers of Ge quantum dots embedded in p-region. The average lateral size of quantum dots was 15 nm and their surface density was about $3\cdot10^{11}$cm^{-2}. Ge quantum dot layers were separated by Si layers. The photosensitive area was equal to $A_d = 10^{-2}$cm^2.

The calculations of generation-recombination noises at different applied voltages for the photodetectors described in Refs. 9 and 49 were done. For the estimation of the model parameters comparison of the calculated dark current-voltage characteristics obtained with the help of the expression (3) with the experimental data from Ref. [9] was carried out. During modelling of temperature dependences of dark current-voltage characteristics, the values of the parameters α and F_0 were fixed as they do not depend on temperature, and the parameters $E_{0,m}$ and $E_{0,n}$ were varied.

Figure 5 shows experimental and theoretical dark current-voltage characteristics of the photodetector with quantum dots of germanium on silicon from Ref. 9 for different temperatures. Theoretical curves in Fig. 5 correspond to the following parameters of the model: $E_{0,m}$ = 40 meV, $E_{0,n}$ = 260–370 meV, F_0 = 6.5 kV/cm, α = 1 meV·cm/kV, σ_E = 10 meV.

It is seen from Fig. 5 that by choosing the appropriate values of activation energies $E_{0,m}$ and $E_{0,n}$ a satisfactory agreement of theoretical predictions with the experimental data is achievable. The behaviour of dark current-voltage characteristics of quantum dot photodetector with the change of the operating temperature is mainly determined by the change in the $E_{0,n}$ value that corresponds to the activation energy for the processes of quantum dots ionization. This behaviour may be caused both by the change in discrete levels position in quantum dot and the change of effective ionization energy of quantum dot due to the change in occupation density of energy levels in quantum dot and barrier level. It is worth mentioning that the obtained value of activation energy of ionization processes due to the barrier tunneling $E_{0,n}$ corresponds well to the energy distance between ground state of the holes and the edge of barrier silicon layer for this photosensitive structure.

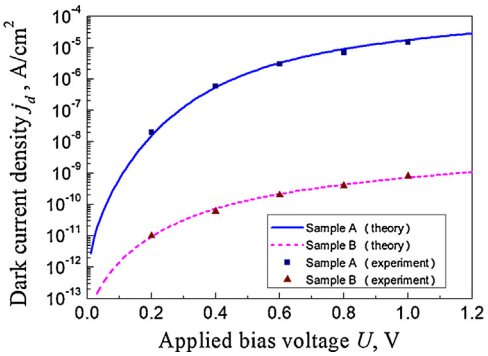

Fig. 6. Dark current density for the photodetectors from Ref. 51 as a function of applied bias U at the temperature $T = 77$ K.

This distance was estimated in Ref. 14 with the help of the theoretical model described in Ref. 52 and is of 272 meV. It should be also noted that the obtained values of the parameter $E_{0,n}$ approximately correspond to the energy distance between ground state of holes in 15 nm quantum dot and the highest level of valence band in silicon (barrier layer) which can be estimated as 360 meV [53]. In accordance with Fig. 5 a conclusion can be made that the dark current model used describes the dependences of the dark current on voltage well enough.

For comparison, in Fig. 5 the theoretical curves corresponding to the model which does not take into account the dispersion of islands by sizes are represented [17]. It seen that the simpler model predicts significantly smaller values of the dark current. So, the conclusion can be made that the homogeneity of islands by sizes is crucial for the enhancement of the quantum dot photodetectors parameters and it is necessary to take the dispersion of islands by sizes into the consideration while modelling the device characteristics of quantum dot structures.

In Refs. 2, and 51 mid infrared photodetectors based on boron-doped *p–i–p*-structures on silicon containing 20 layers of germanium quantum dots in the intrinsic region are described. In these works strong dependence of the dark current on doping level was observed. Figure 6 shows the experimental and calculated dark current-voltage characteristics for the described structures at different dopant concentrations: $6{\cdot}10^{18}$ cm^{-3} (sample A) and $0.6{\cdot}10^{18}$ cm^{-3} (sample B).

The following values of the model parameters were used for the calculations (symbol in brackets denominates the sample type): $F_0 = 2.5$ kV/cm, $\alpha = 1$ meV·cm/kV, $E_{0,m}$ (A) = 70 meV, $E_{0,n}$ (A) = 176 meV, $E_{0,m}$ (B) = 30 meV, $E_{0,n}$ (B) = 244 meV.

It is seen from Fig. 6 that increase in doping level by 10 times results in growth of the dark current by 4–5 orders of magnitude. This effect occurs due to the increase in the density of charge carriers. Such a behavior of the experimental curves (as well as the model parameters) is explained by the change in occupation density of energy levels and Fermi energy level shifting with increase in dopant concentration [2,51].

5. Conclusions

Thus, in this paper the dark current in the structures with quantum dots of germanium on silicon caused by the thermal emission and barrier tunneling, as well as the detectivity of the photodetectors based on such structures are calculated in the supposition of the presence of generation-recombination noises. The presence of the dispersion of quantum dots by sizes is taken in account in the calculations of the generation-recombination noises. It is shown that taking into account the effect of islands array inhomogeneity is crucial for the proper description of the experimental results. For the calculations of the dependencies of quantum dots array parameters on synthesis conditions, the kinetic model of growth of differently shaped quantum dots based on the general nucleation theory is proposed. The comparison of estimated parameters of quantum dots ensembles and calculated dark current-voltage characteristics with the experimental data is carried out, which shows the applicability of the models used. Based on these theoretical models, the calculations of quantum dots parameters and the optimization of the growth conditions in the method of molecular beam epitaxy are carried out for creation of the photodetectors with the improved operating characteristics.

Competing interests

The authors declare that they have no competing interests.

References

[1] D.J. Eaglesham, M. Cerullo, Dislocation-free Stranski–Krastanov growth of Ge on Si(100), Phys. Rev. Lett. 64 (1990) 1943–1946.
[2] Y.-W. Mo, D.E. Savage, B.S. Swartzentruber, M.G. Lagally, Kinetic pathway in Stranski–Krastanov growth of Ge on Si(001), Phys. Rev. Lett. 65 (1990) 1020–1023.
[3] P. Martyniuk, A. Rogalski, Quantum-dot infrared photodetectors: status and outlook, Prog. Quantum Electron. 32 (2008) 89–120.
[4] K. Brunner, Si/Ge nanostructures, Rep. Prog. Phys. 65 (2002) 27–72.
[5] K.L. Wang, D. Cha, J. Liu, C. Chen, Ge/Si self-assembled quantum dots and their optoelectronic device applications, Proc. IEEE 95 (2007) 1866–1882.
[6] A.A. Shklyaev, M. Ichikawa, Extremely dense arrays of germanium and silicon nanostructures, Phys. Usp. 51 (2008) 133–161.
[7] A.V. Voitsekhovskii, A.P. Kokhanenko, A.G. Korotaev, S.N. Nesmelov, Photoelectric characteristics of PtSi-Si Schottky barrier with boron heavily-doped nanolayer, Proc. SPIE 4413 (2001) 387–390.
[8] A. Rogalski, Recent progress in infrared detector technologies, Infrared Phys. Technol. 54 (2011) 136–154.
[9] A.I. Yakimov, Ge/Si heterostructures with Ge quantum dots for mid-infrared photodetectors, Optoelectron. Instrum. Data Proces. 49 (2013) 467–475.
[10] O.P. Pchelyakov, A.V. Dvurechenskii, A.I. Nikiforov, A.V. Voitsekhovskii, D.V. Grigor'ev, A.P. Kokhanenko, Ge/Si nanoheterostructures with ordered Ge quantum dots for optoelectronic applications, Russ. Phys. J. 53 (2011) 943–948.
[11] J. Phillips, Evaluation of the fundamental properties of quantum dot infrared detectors, J. Appl. Phys. 91 (2002) 4590–4594.
[12] A. Rogalski, J. Antoszewski, L. Faraone, Third-generation infrared photodetector arrays, J. Appl. Phys. 105 (2009), 091101.
[13] G. Liu, J. Zhang, L. Wang, Dark current model and characteristics of quantum dot infrared photodetectors, Infrared Phys. Technol. 73 (2015) 36–40.
[14] A.I. Yakimov, V.V. Kirienko, V.A. Armbrister, A.A. Bloshkin, A.V. Dvurechenskii, Phonon bottleneck in p-type Ge/Si quantum dots, Appl. Phys. Lett. 107 (2015), 213502.
[15] A. Mahmoodi, H.D. Jahromi, M.H. Sheikhi, Dark current modeling and noise analysis in quantum dot infrared photodetectors, IEEE Sens. J. 15 (2015) 5504–5509.
[16] H. Liu, Q. Tong, G. Liu, C. Yang, Y. Shi, Performance characteristics of quantum dot infrared photodetectors under illumination condition, Opt. Quant. Electron. 47 (2015) 721–733.
[17] H. Liu, J. Zhang, Performance investigations of quantum dots infrared photodetector, Infrared Phys. Technol. 55 (2012) 3320–3325.
[18] L. Lin, H.L. Zhen, N. Li, W. Lu, Q.C. Weng, D.Y. Xiong, F.Q. Liu, Sequential coupling transport for the dark current of quantum dots-in-well infrared photodetectors, Appl. Phys. Lett. 97 (2010), 193511.
[19] A.V. Osipov, S.A. Kukushkin, F. Schmitt, P. Hess, Phys. Rev. B 64 (1–6) (2001) 205421.
[20] A.V. Osipov, F. Schmitt, S.A. Kukushkin, P. Hess, Stress-driven nucleation of coherent islands: theory and experiment, Appl. Surf. Sci. 188 (2002) 156–162.
[21] V.G. Dubrovskii, G.E. Cirlin, V.M. Ustinov, Kinetics of the initial stage of coherent island formation in heteroepitaxial systems, Phys. Rev. B 68 (1–9) (2003) 075409.
[22] V.G. Dubrovskii, Calculation of the size-distribution function for quantum dots at the kinetic stage of growth, Semiconductors 40 (2006) 1123–1130.
[23] K.A. Lozovoy, A.V. Voytsekhovskiy, A.P. Kokhanenko, V.G. Satdarov, Comparative analysis of pyramidal and wedge-like quantum dots formation kinetics in Ge/Si(001) system, Surf. Sci. 619 (2014) 1–4.
[24] V.G. Dubrovskii, Nucleation Theory and Growth of Nanostructures, Springer, Berlin, DE, 2014, 601 p.
[25] K.A. Lozovoy, A.P. Kokhanenko, A.V. Voitsekhovskii, Influence of edge energy on modeling the growth kinetics of quantum dots, Cryst. Growth Des. 15 (2015) 1055–1059.

[26] P. Muller, R. Kern, The physical origin of the two-dimensional towards three-dimensional coherent epitaxial Stranski–Krastanov transition, Appl. Surf. Sci. 102 (1996) 6–11.
[27] K.A. Lozovoy, A.P. Kokhanenko, A.V. Voitsekhovskii, Generalized Muller–Kern formula for equilibrium thickness of a wetting layer with respect to the dependence of the surface energy of island facets on the thickness of the 2D layer, Phys. Chem. Chem. Phys. 17 (2015) 30052–30056.
[28] C. Ratsch, A. Zangwill, Equilibrium theory of the Stranski–Krastanov epitaxial morphology, Surf. Sci. 293 (1993) 123–131.
[29] V.G. Dubrovskii, N.V. Sibirev, X. Zhang, R.A. Suris, Stress-driven nucleation of three-dimensional crystal islands: from quantum dots to nanoneedles, Cryst. Growth Des. 10 (2010) 3949–3955.
[30] X. Zhang, V.G. Dubrovskii, N.V. Sibirev, X. Ren, Analytical study of elastic relaxation and plastic deformation in nanostructures on lattice mismatched substrates, Cryst. Growth Des. 11 (2011) 5441–5448.
[31] G. Ouyang, L.H. Liang, C.X. Wang, G.W. Yang, Size-dependent interface energy, Appl. Phys. Lett. 88 (1–3) (2006) 091914.
[32] G. Ouyang, C.X. Wang, G.W. Yang, Surface energy of nanostructural materials with negative curvature and related size effects, Chem. Rev. 109 (2009) 4221–4247.
[33] H.T. Johnson, L.B. Freund, Mechanics of coherent and dislocated island morphologies in strained epitaxial material systems, J. Appl. Phys. 81 (1997) 6081–6090.
[34] G.-H. Lu, F. Liu, Towards quantitative understanding of formation and stability of Ge hut islands on Si(001), Phys. Rev. Lett. 94 (1–4) (2005) 176103.
[35] G.-H. Lu, M. Cuma, F. Liu, First-principles study of strain stabilization of Ge(105) facet on Si(001), Phys. Rev. B 72 (1–6) (2005) 125415.
[36] D. Scopece, F. Montalenti, M.J. Beck, Stability of Ge on Si(1 1 10) surfaces and the role of dimer tilting, Phys. Rev. B 85 (1–11) (2012), 085312.
[37] X.L. Li, G.W. Yang, Theoretical determination of contact angle in quantum dot self-assembl, Appl. Phys. Lett. 92 (1–3) (2008) 171902.
[38] X.L. Li, The influence of the atomic interactions in out-of-plane on surface energy and its applications in nanostructures, J. Appl. Phys. 112 (1–7) (2012) 013524.
[39] K.A. Lozovoy, A.V. Voitsekhovskii, A.P. Kokhanenko, V.G. Satdarov, Photodetectors and solar cells with Ge/Si quantum dots parameters dependence on growth conditions, Int. J. Nanotechnol. 12 (2015) 209–217.
[40] K.A. Lozovoy, A.P. Kokhanenko, A.V. Voitsekhovskii, Critical thickness of 2D to 3D transition in Ge_xSi_{1-x}/Si(001) system, Appl. Phys. Lett. 109 (1-4) (2016), 021604.
[41] C.M. Retford, M. Asta, M.J. Miksis, P.W. Voorhees, E.B. Webb, Energetics of {105}-faceted Ge nanowires on Si(001): an atomistic calculation of edge contributions, Phys. Rev. B 75 (1-8) (2007), 075311.
[42] A.B. Talochkin, A.A. Shklyaev, V.I. Mashanov, Super-dense array of Ge quantum dots grown on Si(100) by low-temperature molecular beam epitaxy, J. Appl. Phys. 115 (2014) 144306.
[43] F. Montalenti, D. Scopece, L. Miglio, One-dimensional Ge nanostructures on Si(001) and Si(1 1 10): dominant role of surface energy, C. R. Phys. 14 (2013) 542–552.
[44] A.I. Nikiforov, V.A. Timofeev, S.A. Teys, A.K. Gutakovsky, O.P. Pchelyakov, Initial stage growth of Ge_xSi_{1-x} layers and Ge quantum dot formation on Ge_xSi_{1-x} surface by MBE, Nanoscale Res. Lett. 7 (1-5) (2012) 561.
[45] D.V. Yurasov, Yu.N. Drozdov, The critical thickness of Stranski-Krastanov transition with accounted segregation effect, Semiconductors 42 (2008) 563.
[46] A.I. Yakimov, A.V. Dvurechenskii, A.I. Nikiforov, A.A. Bloshkin, A.V. Nenashev, V.A. Volodin, Electronic states in Ge/Si quantum dots with type-II band alignment initiated by space-charge spectroscopy, Phys. Rev. B 73 (2006) 115333.
[47] J.-M. Baribeau, X. Wu, N.L. Rowell, D.J. Lockwood, Ge dots and nanostructures grown epitaxially on Si, J. Phys. Condens. Matter. 18 (2006) 139.
[48] J. Tersoff, B.J. Spencer, A. Rastelli, H. Kanel, Barrierless formation and faceting of SiGe islands on Si(001), Phys. Rev. Lett. 89 (2002), 196104.
[49] A. Yakimov, V. Timofeev, A. Bloshkin, A. Nikiforov, A. Dvurechenskii, Photovoltaic Ge/Si quantum dot detectors operating in the mid-wave atmospheric window (3 to 5 μm), Nanoscale Res. Lett. 7 (1-6) (2012) 494.
[50] A. Yakimov, V. Kirienko, V. Armbrister, A. Dvurechenskii, Broadband Ge/Si Ge quantum dot photodetector on pseudosubstrate, Nanoscale Res. Lett. 8 (1-5) (2013) 217.
[51] S. Tong, J.-Y. Lee, H.-J. Kim, F. Liu, K.L. Wang, Ge dot mid-infrared photodetectors, Opt. Mater. 27 (2005) 1097–1100.
[52] A.I. Yakimov, A.A. Bloshkin, A.V. Dvurechenskii, Calculating the energy spectrum and electronic structure of two holes in a pair of strained Ge-Si coupled quantum dots, Phys. Rev. B 81 (1–11) (2010) 115434.
[53] A.I. Yakimov, N.P. Stepina, A.V. Dvurechenskii, A.I. Nikiforov, A.V. Nenashev, Interband absorption in charged Ge/Si type-II quantum dots, Phys. Rev. B 63 (1–6) (2001), 045312.